Journal of Cardiovascular Disease Research

ISSN: 0975-3583, 0976-2833 VOL 14, ISSUE 08, 2023

Green Synthesis of Silver Nanoparticles from Sarcopharyngia ventricosa

E. Nirmala[1], Prof. Dr. Dillip Kumar Brahma[2], Balan Paramasivam[3], Shivani Singh[4], Namrata[5], D.T. Sakhare[6], Mohit Chadha[7], Nihar Ranjan Kar [8], Manisha Masih Singh*

1. Vice Principal, Shri Venkateshwara College Of Pharmacy, Ariyur, Puducherry 605102
2. Principal & Professor, Department Of Pharmacy, NSIP, Netaji Subhas University (NSU), 831001
3. Professor, The Erode College Of Pharmacy, Veppampalayam, Vallipurathanpalayam, Tamilnadu Po. Erode-638112,
4. Research Associate, Chhatrapati Shahu Ji Maharaj University, Kanpur,Uttar Pradesh 208017
5. Assistant Professor, Kc Institute Of Pharmaceutical Sciences
6. Assistant Professor, U.G.,P.G. & Research Centre, Department Of Chemistry, Shivaji Art's, Comm. & Science College Kannad Dist Aurangabad 431103 Maharashtra India
7. Associate Professor, Baba Farid College of Pharmacy, Morkarima, Mullanpur (Distt. Ludhiana) Pin Code 142023
8. Assistant Professor, Centurion University of Technology And Management, Gopalpur, Balasore, Odisha, India, Pin-756044
9. Associate Professor, School Of Pharmacy Cec Lal Khadan, Masturi Jairamnagar Road, Bilaspur Cg-495004

Corresponding: Dr Manisha Masih Singh
manishamasih85@Gmail.Com
Affiliation: *Associate Professor, School Of Pharmacy Cec Lal Khadan, Masturi Jairamnagar Road, Bilaspur Cg-495004*

Abstract:

Green syntheses of metallic nanoparticles using plant extracts as effective sources of reductants and stabilisers have acquired some momentum due to their non-toxicity, environmental friendliness, and rapidity. The current study demonstrates how to harvest aerial parts of Anthemis pseudocotula Boiss to create silver nanoparticles (AP-AgNPs) quickly, affordably, and sustainably. The AP aerial parts extract in this instance worked as a stabilising and reducing agent. The green AP-AgNPs that were synthesised were examined using a number of techniques, including XRD, UV-Vis, FT-IR, TEM, SEM, and EDX. The antimicrobial and antibiofilm activity of as-prepared AP-AgNPs against a variety of Gram-positive and Gram-negative bacterial strains as well as fungi, including Escherichia coli, Staphylococcus aureus, multidrug-resistant Pseudomonas aeruginosa, and Acinetobacter baumannii, was tested using a standard two-fold microbroth dilution method and tissue culture plate The antimicrobial activity data unmistakably shown that the Gram-negative bacterium MDR-PA was more negatively influenced by AgNPs when compared to other

ISSN: 0975-3583, 0976-2833 VOL 14, ISSUE 08, 2023

Gram-negative, Gram-positive, and the fungus C. albicans. Gram-negative bacteria like MDR-PA, E. coli, and MDR-AB are prevented from developing biofilms by AgNPs at 0.039 mg/mL by 78.98 1.12, 65.77 1.05, and 66.94 1.35%, respectively. However, at the same dose (i.e., 0.039 mg/mL), AP-AgNPs inhibits the formation of biofilms generated by Gram-positive bacteria like MRSA, S. aureus, and the fungus C. albicans by 67.81 0.99, 54.61 1.11, and 56.22 1.06%, respectively. The findings of the present investigation demonstrate that greenly synthesised AP-AgNPs are efficient antibacterial and antibiofilm agents against certain bacterial and fungal species.

Key Words: XRD, UV-Vis, FT-IR, TEM, SEM, and EDX.

Introduction

Nanotechnology can offer solutions to numerous environmental and technical chal- lenges in the areas of medicine, agriculture, food, electronics and wastewater treatment. From the past few decades, there has been an augmented importance on the development of metal nanoparticles owing to their remarkable optical and electrical properties. Excellent physico-chemical and physico-mechanical properties of metal nanoparticles have made them desirable aspirants for innovative applications in the medical field as antibiotic and anticancer agents . In this context, noble metal nanoparticles such as platinum, copper, silver, gold, palladium, magnesium, zinc, and titanium, have attained significant consideration for medical applications due to their multifunctional capabilities. However, physical approaches are preferred for the synthesis of high-quality metal nanoparticles, in the efforts to diminish toxic waste. Increasingly, considerable interests have been developed towards the advancement of novel wet-synthesis approaches which are efficient, inexpensive and can be easily perform by using eco-friendly reagents including natural products, etc.[1] Natural products, termed as phytomolecules acquired from fungi, bacteria and plants have demonstrated excellent reducing potential during the preparation of metal nanopar- ticles due to substantial diversities in their chemical compositions. Due to their reducing abilities, the active phytomolecules existing in the plant extracts not only fa- cilitate the synthesis of nanomaterials but also assist in the stabilization of the surface of resulting nanoparticles during the synthesis. [2] Furthermore, it has also been confirmed by various studies that plant extracts containing bioactive secondary metabo- lites like tannins, terpenoids, polyphenols,

ISSN: 0975-3583, 0976-2833 VOL 14, ISSUE 08, 2023

alkaloids, amines, polysaccharides, ketones and aldehydes, flavonoids, lignin and proteins, etc., play the dual role as reducing and stabilizing agents in the conversion of metal ions into metal nanoparticles. For ex- ample, *Origanum vulgare* L., *Pulicaria glutinosa*, *Cordia myxa*, etc. have been employed for the synthesis of a variety of nanoparticles, which have been selected based on their phy- tochemical composition. [3] Often, nanomaterials obtained by using plant extracts have been used for a variety of biomedical applications such as antimicrobial, anti-fungal agents, even as biosensors and for several other biological applications. [4] Recently, *Aegle marmelos* aqueous leaf extract was used to prepare Ag NPs which have demonstrated good antimicrobial activity against *Bacillus megaterium*, *Bacillus aryabhattai*, *Staphylococcus aureus*, *Serratia marcescens* and *Pseudomonas putida*. In this case, the highest zone formation was observed at (8.4 0.3) in 100 µg/mL concentration of Am-AgNPs against *Serratia marcescens*. Although silver nanoparticles have been extensively studied earlier, their synthesis with different media may produce a diverse quality of nanoparticles with different sizes, shapes, and compositions etc. These properties may have a significant effect on the resulting biological potential of the material. Therefore, it is beneficial to test the biological properties of NPs prepared with different sources of reagents. In this scenario, one such plant *Sarcopharyngia ventricosa*. has not been investigated for the synthesis of silver nanoparticles and an exploration of their biological potential. *Sarcopharyngia ventricosa* belongs to the family Asteraceae and is known to possess a variety of active phytochemicals such as sesquiterpene lactones, flavonoids and polyacetylenes.[4] Among different metallic nanoparticles, silver have been extensively utilized in var- ious fields, including as an anti-microbial agent in different functional materials, as a potent coating agent, effective biosensors and as a catalyst in various chemical reactions. Furthermore, silver nanoparticles have also been known to possess effective biological properties such as anti-platelets and anti-HIV etc.,. [5] Hence, in the present study, we report the synthesis of silver nanoparticles (AP-AgNPs) using the aerial part extract of *Sarcopharyngia ventricosa* plant. The synthesized AP-AgNPs were characterized using several techniques such as XRD, UV-Vis, FT-IR, TEM, SEM, and EDX. In addition, during this study, antimicrobial and anti-biofilm properties of the as-prepared green synthesized AP-AgNPs were evaluated by using selected bacterial and fungal strains. [6]

Materials and Methods:

ISSN: 0975-3583, 0976-2833 VOL 14, ISSUE 08, 2023

Plant Collection: Silver nitrate, triethylamine, MTT (3-[4,5-dimethylthiazol-2-yl]-2,5-diphenyltetrazolium bromide), dimethyl sulfoxide, acridine orange, ethidium bromide, Dulbecco's Modified Ea- gle Medium (DMEM), fetal bovine serum (FBS), trypsin-EDTA (ethylenediaminetetraacetic acid) solution, antibiotic-antimycotic solution, nutrient broth, and nutrient agar were pro- cured from HiMedia Laboratories Pvt. Ltd., Maharashtra, India. B16F10 murine melanoma cell lines were procured from NCCS, India. Escherichia coli, Staphylococcus aureus, and Pseudomonas aeruginosa were procured from CSIR-IMTECH, India. Leaves and stems from adult Sarcopharyngia ventricosa plants (~12–15 m in height) grown in the wild were collected. A combination of emergent, young, and mature leaves and stems were collected for analysis. The plant sample was taxonomically identified by the herbarium curator, and a voucher specimen (18222) was deposited at the Ward herbarium, School of Life Sciences, University of KwaZulu-Natal.

Plant Collection

Extraction of Plant Leaves: Extract Fresh leaves of Plectranthus amboinicus were obtained. A total of 10 g of fresh leaves were cleaned using deionized water to eliminate impurities and dust particles. Plectranthus amboinicus leaves were minced into small pieces. They were soaked in 50 mL of deionized water. [7] The contents were allowed to boil at 60^{O}C for 30 min. The solution contents were subjected to centrifugation for 10 min at 4000 rpm. The plant extract was kept at 4^{O}C until it was utilized for further experiments (Figure 1)

Figure 1: Extraction of Plant Leaves

ISSN: 0975-3583, 0976-2833 VOL 14, ISSUE 08, 2023

Reflux Solvent Extraction: Crude methanolic leaf and stem extracts were prepared through reflux extraction using analytical grade (AR) methanol at a ratio of 10 g powdered material to 100 mL solvent. A round-bottom flask was heated (60 ◦C) by a reflux extraction, and the extraction proceeded for 3 h. The solutions were filtered (Whatman No. 1); after each extraction, the extract was retained; and the procedure was repeated twice. Following three extractions, the resulting leaf and stem extracts for each solvent were vacuum-filtered using Whatman No. 1 until no precipitate was observed, stored separately in air-tight sterilized glass jars, and kept in a dark room, at 4 ◦C, until further use. [8]

Synthesis of AgNPs: The AgNPs were photosynthesized by adding 1 ml (2%) of CSE concentrate into a round bottom flask containing a 49 ml aqueous solution comprising 85 mg of silver nitrate (0.5 mM). The pH value of the mixture was adjusted to 7. The experiment was replicated to assess the effect of the concentration of plant extract on the yield and characteristics of nanoparticles by using different concentrations (4, 8, and 16%) of CSE. The above procedure was repeated using PAE, Table 1. UV-vis absorbance was taken immediately after mixing the plant extract and silver nitrate solution. For further absorbance reading, 5 ml from each sample was dispensed into 15 ml falcon tubes and kept in a dark cupboard. The round-bottomed flasks were placed in a dark cabinet and left to stand for 24 h, after which each was equipped with a magnetic stir bar and fixed with a cooling condenser. The reaction mixture was left to stand for 2 h at 85°C, then left to cool down at room temperature followed by centrifuging at 9,000 rpm for 30 min. The sediment obtained was washed numerous times with distilled de-ionized water after which the final precipitate produced was dried at 80°C in an oven for 12 h. [9]

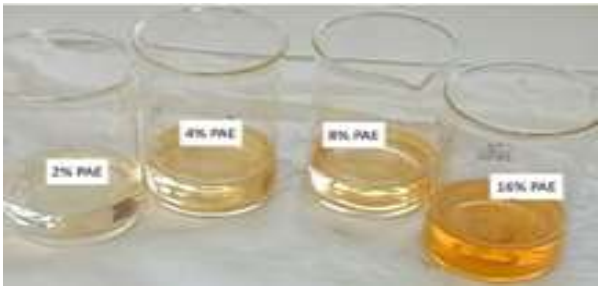

Concentration of	Volume of plant	Volume of silver	Total volume (ml)

ISSN: 0975-3583, 0976-2833 VOL 14, ISSUE 08, 2023

Prunus africana extract (%)	extract (ml)	nitrate (ml)	
2	1	49	50
4	2	48	50
8	4	46	50
16	8	42	50

Table 1: Concentration of plant extract, volume of plant extract, and volume of silver nitrate used to green synthesize AgNPs.

UV-Visible Spectral Analysis: This was achieved using a Cary 5000 UV Vis-NIR Spectrophotometer, Agilent Technologies. The samples were examined by UV-vis spectroscopy operating at a resolution of 1 nm between 190 and 800 nm ranges to analyze the optical property of biosynthesized AgNPs. Absorbance was read at 0 min, 0.5, 1, 2, 3, 4, and 5 h for different concentrations of CSE-AgNO3 solution and at 0 min, 0.5, 1, 2, 3, 4, 6, 8, 10, 12, 24, and 72 h for PAE-AgNO3 mixtures. [10]

Preparation, Purification, and Quantification of Samples: The six solutions of synthesised silver nanoparticles (AgNPs), namely leaf methanol (LM), fresh leaf (FL), powdered leaf (PL), stem methanol (SM), fresh stem (FS), and powdered stem (PS), were thereafter subjected to three rounds of centrifugation at 10,000 revolutions per minute (rpm) for a duration of 30 minutes each at a temperature of 4 degrees Celsius. This process was carried out utilising a BECKMAN COULTER Avanti®J-E centrifuge located in Indianapolis, IN, USA. After the centrifugation process, a volume of 20 mL of distilled water was used to cleanse the pellet in order to eliminate any residual substances, such as contaminated plant debris, solution biomolecules, and cellular metabolites. The suspensions were subsequently dried in an oven set to 50°C on three separate occasions during the washing process. The yield of the synthesised silver nanoparticles (AgNPs) was determined over a period of about seven days. The desiccated silver nanoparticles (AgNPs) were rehydrated using sterile distilled water in order to facilitate further analysis. [11]

Sarcopharyngia ventricosa and AgNPs Silver Nanoparticles Characterization:

ISSN: 0975-3583, 0976-2833 VOL 14, ISSUE 08, 2023

Scanning Electron Microscopy (SEM): The size and morphology of the biosynthesized AgNPs were examined by field emission scanning electron microscopy (FESEM), a Carl Zeiss SIGMA model operated at 5 kV. Briefly, a thin film of AgNPs was prepared by spreading 1 mg of each sample on carbon tape followed by coating it with carbon. Surface images were captured at different magnifications. ImageJ software was used to estimate the size distribution of AgNPs.

Energy-Dispersive X-ray (EDX) Analysis: About 500 mg of green synthesized AgNPs powder were analyzed with a powder X-ray diffraction (XRD) employing BRUKER AXS diffractometer, D8 Advance (Germany) fitted with Cu-Ka radiation (λKα1:1.5406 Å) from 2θ 0.5° –130° , with increment of Δ2θ: (0.034°), voltage of 40 kV, current of 40 mA, power of 1.6 kW, and counting time of 0.5 s/step. Generated data was analyzed by OriginPro and resultant peaks two theta values were compared with the standard AgNPs values from the International Center for Diffraction Data (ICDD) database. [12]

Fourier Transform Infrared (FTIR) Spectral Analysis: Fourier transform infrared spectroscopy with a PerkinElmer Spectrum RX I Fourier transform IR system with a frequency ranging from 400 to 4,000 cm−1 and a resolution of 4cm−1 and set to perform at least 64 scans per sample was used to investigate the organic functional groups of the plant extracts used in the bio-reduction of silver nitrate to silver nanoparticles as follows: 2 mg of silver nanoparticles and 2 g of potassium bromide (KBr) were desiccated at 200° C under reduced pressure overnight. The dried silver nanoparticles were standardized with 100 mg of KBr and then hard-pressed to form very thin transparent circular pellets. The pellets were screened at 4,000–400 cm−1 Wavenumber range. A KBr pellet was used to plot the baseline. [13]

Results and Discussion

Visual Inspection of Synthesized AgNPs: The visual confirmation of synthesized AgNPs using leaf methanol (LM), stem methanol (SM), fresh leaf (FL), fresh stem (FS), powdered leaf (PL), and powdered stem (PS) extracts of Sarcopharyngia ventricosa was visually evident in terms of the color variation of the reaction solutions. The methanol suspensions (extract + AgNO3 before incubation) of Sarcopharyngia ventricosa displayed a greenish solution for the leaves and a murky yellow coloration for the stems (Figure 1-1A). The fresh suspensions (extract + AgNO3 before incubation) for the leaves appeared pale yellow, and the stem solution was colorless.

ISSN: 0975-3583, 0976-2833 VOL 14, ISSUE 08, 2023

While the powdered leaf and stem suspensions (extract + AgNO3 before incubation) both displayed a bright yellow color (Figure 1-1C). However, after the addition of AgNO3 and the incubation period for 3 h at 80 ◦C, all solutions revealed a color change, except for the synthesized AgNPs using fresh stem extracts. The synthesized AgNPs using leaf and stem methanolic extracts turned deep brown/ruby brown (Figure 1-2A). Interestingly, the synthesized AgNPs using fresh stem extracts did not display any prominent color changes and appeared extremely pale yellow in coloration (Figure 1-2B); however, the fresh leaf extracts appeared murky brown. The synthesized AgNPs using powdered leaf and stem extracts both appeared dark brown and golden brown, respectively. [14]

UV-Visible Spectroscopy: In order to ascertain the production, distribution, and stability of synthesised AgNPs in a solution, UV-visible absorption spectra are often used in their verification and characterisation. The current study investigated the biological production of AgNPs using a variety of extracts (methanol, fresh, and powder) produced from Sarcopharyngia ventricosa's leaves and stems. The surface plasmon resonance (SPR) of the resultant solutions was then examined throughout a wavelength range of 300 to 700 nm. Within the wavelength range of 400-460 nm, prominent silver (Ag) surface plasmon resonance (SPR) bands are frequently detected. The UV absorption spectra of the synthesised silver nanoparticles (AgNPs) are shown in Figure 2. All silver nanoparticles (AgNPs) showed variable-type absorption bands. In the current investigation, synthesised AgNPs were extracted using several solvents, including leaf methanol (LM), stem methanol (SM), fresh leaf (FL), fresh stem (FS), powdered leaf (PL), and powdered stem (PS). SPR bands were detected at wavelengths of 418, 418, 478, 364, 446, and 414 nm. The synthesised AgNPs using leaf methanol (LM) had the greatest maximum absorbance value of 1.824, followed by stem methanol (1.599), powdered leaf (1.036), powdered stem (0.832), and fresh leaf (0.521). The fresh stems had the lowest absorption (0.123). All synthetically produced silver nanoparticles, with the exception of those made from fresh leaves, had wavelengths that fell within the range of silver nanoparticle surface plasmon resonance (SPR) bands. The development of peaks at roughly 420 nm indicates that earlier studies using T. divaricata extracts for the production of AgNPs had variable results. In contrast, the current research discovered a wide variety of peaks, as shown in Figure 2. Additionally, Vinodhini et al.'s recent study on T. divaricata extracts found a strong absorption band at 426 nm, which is

ISSN: 0975-3583, 0976-2833 VOL 14, ISSUE 08, 2023

suggestive of the synthesis of AgNPs. Additionally, as shown in Figure 2, the properties of elongated tails suggest changes in the size distribution of the synthesised nanoparticles. [15]

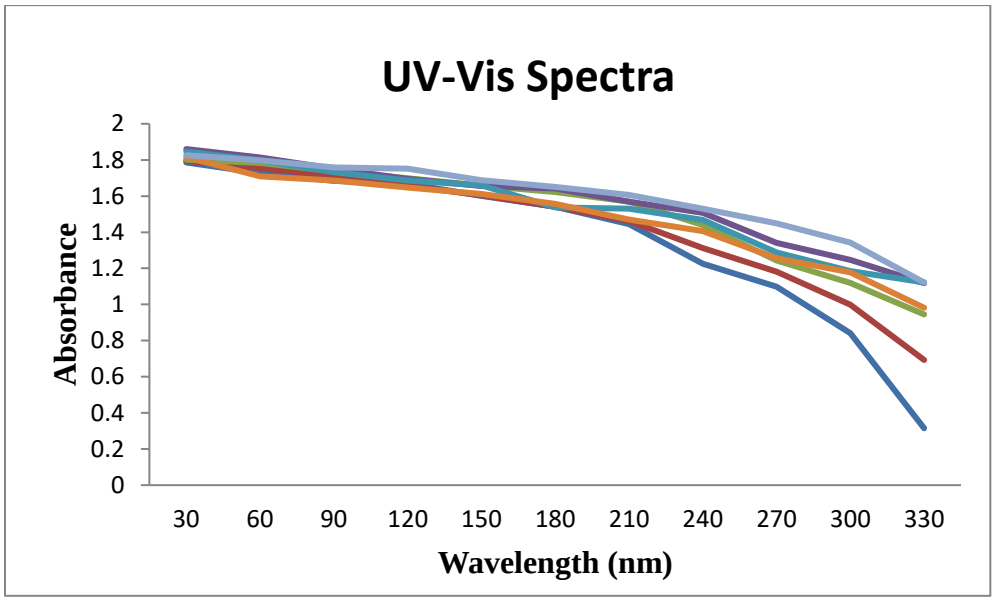

Figure 2: UV-vis spectra of AgNPs synthesized using leaf and stem

Quantification of Synthesized AgNPs: The yield for synthesized AgNPs using leaf and stem extracts (methanol, fresh, and powder) of Sarcopharyngia ventricosa was extremely low (Table 1). The highest percentage yield was observed for AgNPs synthesized using powdered leaf extracts (1.638%), followed by powdered stem extracts (1.190%).[16] The AgNPs synthesized using methanol stem (0.737%) and methanol leaf extracts (0.659%) displayed the second-highest percentage yield, whereas the AgNPs synthesized using fresh leaves (0.023%) and fresh stems extracts (0.027%) showed the lowest percentage yield. The variable percentage yield for the synthesized AgNPs using various extracts could be attributed to several factors such as the plant organ used, preparation of plant material (dehydration), quantity and type of bioactive compounds present within extracts, temperature, and incubation time. [17]

Extracts	Leaves	Stems	Leaves	Stems
	Dried Extract Yield (g)		Yield (%)	
Fresh extract	0.008	0.007	0.017	0.023
Powdered extract	0.182	0.123	1.832	1.201

ISSN: 0975-3583, 0976-2833 VOL 14, ISSUE 08, 2023

Methanol Extract	0.052	0.069	0.599	0.642

Table 1: Percentage yield of the synthesized AgNPs

Scanning Electron Microscopy (SEM): Scanning electron microscopy (SEM) was employed to analyse and authenticate the morphology and overall particle size of the synthesised silver nanoparticles (AgNPs) derived from various extracts of Sarcopharyngia ventricosa. The SEM images presented in Figures 3 provide evidence for the generation and particle size (100 nm) of the AgNPs. The AgNPs were mostly spherical in form, displaying homogeneity, and shown significant agglomeration during the manufacturing process. Devaraj et al. conducted a study that explored the production of silver nanoparticles (AgNPs) using extracts derived from T. divaricata. The synthesised silver nanoparticles (AgNPs) exhibited a constant spherical shape, with sizes ranging from 29 to 68 nm (100 nm) as observed using scanning electron microscopy (SEM). However, in comparison to the particles investigated in the present study, the synthesised particles had a more uniform dispersion and showed less agglomeration. In a separate study conducted by Vinodhini et al., the use of T. divaricata in the synthesis of AgNPs resulted in agglomeration to some extent. However, the nanoparticles exhibited distinct rod-like structures with an average size ranging from 40 to 57 nm. The process of dehydrating or drying the synthesised solutions is expected to result in agglomeration. Furthermore, empirical studies have revealed that variations in reaction temperature, extract concentration, bioactive compounds, and AgNO3 concentration often exert an influence on the extent of agglomeration and average particle size of AgNPs. [18]

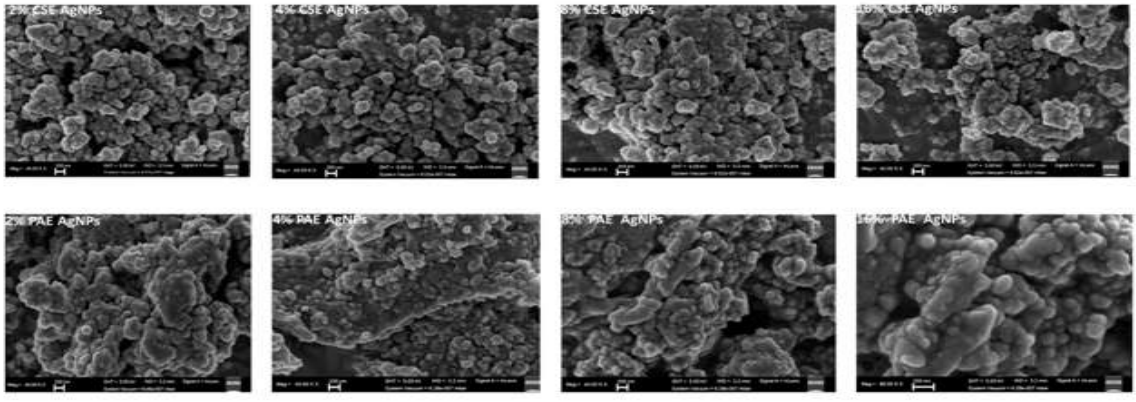

Figure 4: Scanning Electron Microscopy (SEM)

ISSN: 0975-3583, 0976-2833 VOL 14, ISSUE 08, 2023

Energy-Dispersive X-ray (EDX) Analysis: Te crystalline nature of biogenic nanoparticles was confrmed by X-ray crystallography, recorded on a Panalitycal X'pert Pro MRD X-ray difraction instrument, with Cu Kα radiation (λ=0.15418 nm) over the scanning range 2θ=30°–80°, with a step of 0.02 degree. Te XRD pattern of the synthesized AgNPs, shows several peaks, where the four main peaks located at 38.10°, 44.20°, 64.41° and 77.39°, corresponding to the (111), (200), (220) and (311) planes, respectively, to the facets of face-centered cubic (fcc) crystal structure of silver (JCPDS, No. 04-0783). An intense peak, located at 32.15° could be indexed to a cubic structure of AgK3 (PDF 50-1435). Te presence of K was further confrmed during XPS and EDS experiments. [19]

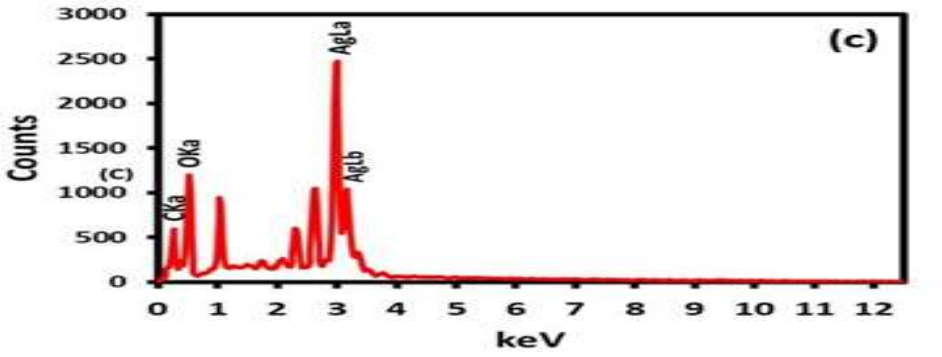

Figure 5: Energy-Dispersive X-ray (EDX) Analysis

Fourier Transform Infrared (FTIR) Spectroscopy: The FTIR spectroscopy measurements were undertaken to determine the biomolecules that are likely responsible for the reduction of Ag ions and the capping of the bio-reduced AgNPs produced by the leaf and stem extracts of Sarcopharyngia ventricosa. The FTIR spectra displayed different stretches and bending of bonds at various peaks for all synthesized AgNPS using leaf methanol (LM), stem methanol (SM), fresh leaf (FL), fresh stem (FS), powdered leaf (PL), and powdered stem (PS) extracts due to the presence of different bioactive compounds in the above treatments. However, the observed peak patterns were very similar across all AgNPs produced, with a few significant differences in peaks observed for certain AgNPs. The FTIR spectra displayed strong intensity peaks between 3200 cm−1 and 3400 cm−1 for all AgNP solutions. These peaks correspond to the strong broad O–H stretch of alcohols, C–H stretch of alkynes, C=O, C–O, O–H stretching of carboxylic acids, and H–bonded to phenols, whereas the bands observed between 2922 cm−1 and 2936 cm−1 correspond to the medium C–H stretch of alkanes and the strong broad N–H stretch of amine

ISSN: 0975-3583, 0976-2833 VOL 14, ISSUE 08, 2023

salts [41,59]. Strong peaks displayed by bands from regions between 2339 cm−1 and 2395 cm−1 resemble O=C=O carbon dioxide stretching; however, bands in the 2100 cm−1 to 2140 cm−1 region represent weak C≡C alkyne stretching . Interestingly, the compound group isothiocyanate N=C=S showed strong stretching at 2095.91 cm−1 (FL) and 2091.37 cm−1 (FS) in fresh extracts only. The sharp peaks from 1588.93 cm−1 to 1623.91 cm−1 indicate C=C, C–O, and N–H stretching to alkenes and amines. The C–H plane bends to alkanes and aldehydes, C–O and O–H medium/strong stretches, bending of alcohols and phenols, CO–O–CO strong broad stretching of anhydrides, and strong S=O stretches of sulfoxide and sulfonate/sulfonamide all correspond to the 1043 cm−1–1384 cm−1 region. The medium peaks at 690 cm−1–895 cm−1 correspond to medium C=C bending of alkenes and strong C–l halo compounds. The observed FTIR spectra indicated the presence of a variety of functional groups at varying positions. The results suggest that the capping of the NPs may contain phenolic and terpenoid compounds, with functional groups of carboxylic acids, alcohols, alkanes, and esters, which may have been influenced by the different treatments (various solvents and ratios of the leaf and stem material) and have reduced AgNO3 to AgNPs using a variety of bioactive compounds. The results of the present study are consistent with Vinodhini et al.; however, additional research regarding which compound is responsible for capping is require. Furthermore, the occurrence of medium-intensity peaks in the amide region, more specifically the amide I (one) area, also suggests that proteins/enzymes are likely responsible for the reduction of Ag ions for the synthesis of AgNPs. According to the results of this study, the occurrence of proteins may be accountable for the formation of a thin film (cap) surrounding the AgNPs. Studies have confirmed that amino acid residues and peptides of proteins usually coat AgNPs to prevent the agglom eration of particles, allowing the stability of NPs in solution. In addition, the occurrence of impurities may be attributed to other organic substances in the various plant extracts. [20]

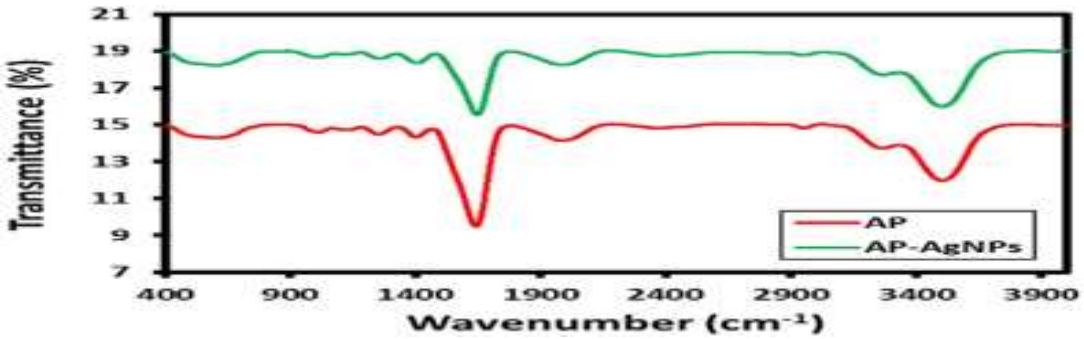

ISSN: 0975-3583, 0976-2833 VOL 14, ISSUE 08, 2023

Conclusions: The use of a green approach for AgNP biosynthesis has garnered significant attention due to its effectiveness, cost-effectiveness, environmental sustainability, and safety. This study utilised several Sarcopharyngia ventricosaextracts to successfully show the environmentally friendly production of silver nanoparticles (AgNPs). [21] The resulting nanoparticles exhibited a range of morphologies, including spherical, ovate, and triangular, with sizes ranging from 16.06 nm to 80.26 nm. The presence of biological components in the leaf and stem extracts is believed to be responsible for the capping and stability of the synthesised Ag ions in the solution. Groups such as alcohols, phenolics, aldehydes, alkanes, amines, and aromatic compounds can be identified as examples. Future research should focus on the identification of the specific biochemical constituents present in Sarcopharyngia ventricosathat are responsible for the synthesis of silver nanoparticles (AgNPs). This investigation represents the initial exploration into the production and characterization of AgNPs derived from Sarcopharyngia ventricosa. [22]

References:

1. Agnihotri, S., Mukherji, S., and Mukherji, S. (2013). Immobilized Silver Nanoparticles Enhance Contact Killing and Show Highest Efficacy: Elucidation of the Mechanism of Bactericidal Action of Silver. *Nanoscale* 5 (16), 7328–7340. doi:10.1039/c3nr00024a
2. Ajitha, B., Ashok Kumar Reddy, Y., and Sreedhara Reddy, P. (2015). Green Synthesis and Characterization of Silver Nanoparticles Using Lantana Camara Leaf Extract. *Mater. Sci. Eng. C* 49, 373–381. doi:10.1016/ j.msec.2015.01.035
3. Akintelu, S. A., Bo, Y., and Folorunso, A. S. (2020). A Review on Synthesis, Optimization, Mechanism, Characterization, and Antibacterial Application of Silver Nanoparticles Synthesized from Plants. *J. Chem.* 2020, 3189043. doi:10.1155/2020/3189043
4. Albrecht, M. A., Evans, C. W., and Raston, C. L. (2006). Green Chemistry and the Health Implications of Nanoparticles. *Green. Chem.* 8 (5), 417–432. doi:10.1039/b517131h
5. Anandalakshmi, K., Venugobal, J., and Ramasamy, V. (2016). Characterization of Silver Nanoparticles by green Synthesis Method Using Pedalium Murex Leaf Extract and Their Antibacterial Activity. *Appl. Nanosci.* 6 (3), 399–408. doi:10.1007/s13204-015-0449-z

ISSN: 0975-3583, 0976-2833 VOL 14, ISSUE 08, 2023

6. Bin Sayeed, M., Karim, S., Sharmin, T., and Morshed, M. (2016). Critical Analysis on Characterization, Systemic Effect, and Therapeutic Potential of Beta- Sitosterol: a Plant-Derived Orphan Phytosterol. *Medicines* 3 (4), 29. doi:10.3390/medicines3040029
7. Bondarenko, O., Juganson, K., Ivask, A., Kasemets, K., Mortimer, M., and Kahru, A. (2013). Toxicity of Ag, CuO and ZnO Nanoparticles to Selected Environmentally Relevant Test Organisms and Mammalian Cells *In Vitro*: a Critical Review. *Arch. Toxicol.* 87 (7), 1181–1200. doi:10.1007/s00204-013- 1079-4
8. Botten, D., Fugallo, G., Fraternali, F., and Molteni, C. (2015). Structural Properties of Green Tea Catechins. *J. Phys. Chem. B* 119 (40), 12860–12867. doi:10.1021/ acs.jpcb.5b08737
9. Carbin, B.-E., Larsson, B., and Lindahl, O. (1990). Treatment of Benign Prostatic Hyperplasia with Phytosterols. *Br. J. Urol.* 66 (6), 639–641. doi:10.1111/j.1464- 410x.1990.tb07199.x
10. Castillo-Henríquez, L., Alfaro-Aguilar, K., Ugalde-Álvarez, J., Vega-Fernández, L., Montes de Oca-Vásquez, G., and Vega-Baudrit, J. R. (2020). Green Synthesis of Gold and Silver Nanoparticles from Plant Extracts and Their Possible Applications as Antimicrobial Agents in the Agricultural Area. *Nanomaterials* 10 (9), 1763. doi:10.3390/nano10091763
11. Castro, L., Blázquez, M. L., Muñoz, J. á., González, F. G., and Ballester, A. (2014). Mechanism and Applications of Metal Nanoparticles Prepared by Bio- Mediated Process. *Rev. Adv. Sci. Engng* 3 (3), 199–216. doi:10.1166/ rase.2014.1064
12. CDC (2013). *Antibiotic Resistance Threats in the United States*. U. S. Department of Health and Human Services, Centers for Disease Control and Prevention.
13. Chattopadhyay, S., Dash, S. K., and Ghosh, T. (2010). Surface modification of cobalt oxide nanoparticles using phosphonomethyl iminodiacetic acid followed by folic acid: a biocompatible vehicle for targeted anticancer drug delivery. *Cancer Nano.* 4, 103–116. doi:10.1007/s12645-013-0042-7
14. Das, R., Nath, S. S., Chakdar, D., Gope, G., and Bhattacharjee, R. (2010). Synthesis of Silver Nanoparticles and Their Optical Properties. *J. Exp. Nanoscience* 5 (4), 357–362. doi:10.1080/17458080903583915
15. Dickson, J. S., and Koohmaraie, M. (1989). Cell Surface Charge Characteristics and Their Relationship to Bacterial Attachment to Meat Surfaces. *Appl. Environ. Microbiol.* 55 (4), 832–836. doi:10.1128/aem.55.4.832-836.1989

ISSN: 0975-3583, 0976-2833 VOL 14, ISSUE 08, 2023

16. Durán, N., Nakazato, G., and Seabra, A. (2016). Antimicrobial Activity of Biogenic Silver Nanoparticles, and Silver Chloride Nanoparticles: an Overview and Comments. *J Appl. Microbiol. Biotechnol.* 100 (15), 6555–6570. doi:10.1007/ s00253-016-7657-7
17. ECDC (2018). "European Centre for Disease Prevention and Control; Antimicrobial Resistance Surveillance in Europe 2017," in *Annual Report of the European Antimicrobial Resistance Surveillance Network (EARS-Net)* (Stockholm: ECDC). doi:10.2900/797061
18. Jafari, A., Jafari Nodooshan, S., Safarkar, R., Movahedzadeh, F., Mosavari, N., Novin Kashani, A., et al. (2018). Toxicity Effects of AgZnO Nanoparticles and Rifampicin on *Mycobacterium tuberculosis* into the Macrophage. *J. Basic Microbiol.* 58 (1), 41–51. doi:10.1002/jobm.201700289
19. Jameel, M. S., Aziz, A. A., and Dheyab, M. A. (2020). Green Synthesis: Proposed Mechanism and Factors Influencing the Synthesis of Platinum Nanoparticles %. *J. Green. Process. Synth.* 9 (1), 386–398. doi:10.1515/gps-2020-0041
20. Kagithoju, S., Godishala, V., and Nanna, R. S. (2015). Eco-friendly and green Synthesis of Silver Nanoparticles Using Leaf Extract of Strychnos Potatorum Linn.F. And Their Bactericidal Activities. *3 Biotech.* 5 (5), 709–714. doi:10.1007/ s13205-014-0272-3
21. Kampa, M., Alexaki, V.-I., Notas, G., Nifli, A.-P., Nistikaki, A., Hatzoglou, A., et al. (2004). Antiproliferative and Apoptotic Effects of Selective Phenolic Acids on T47D Human Breast Cancer Cells: Potential Mechanisms of Action. *Breast Cancer Res.* 6 (2), R63. doi:10.1186/bcr752
22. Kelly, K. L., Coronado, E., Zhao, L., and Schatz, G. C. (2003). The Optical Properties of Metal Nanoparticles: The Influence of Size, Shape, and Dielectric Environment. J. Phys. Chem. B 107 (3), 668–677. doi:10.1021/ jp026731y